A mesoscale phytoplankton bloom in the polar Southern Ocean stimulated by iron fertilization

Philip W. Boyd[1], Andrew J. Watson[2], Cliff S. Law[3], Edward R. Abraham[4], Thomas Trull[5], Rob Murdoch[4], Dorothee C. E. Bakker[2], Andrew R. Bowie[6,3], K. O. Buesseler[7], Hoe Chang[4], Matthew Charette[7], Peter Croot[8], Ken Downing[4], Russell Frew[9], Mark Gall[10], Mark Hadfield[4], Julie Hall[11], Mike Harvey[4], Greg Jameson[3], Julie LaRoche[12], Malcolm Liddicoat[3], Roger Ling[3], Maria T. Maldonado[13,14], R. Michael McKay[15], Scott Nodder[4], Stu Pickmere[11], Rick Pridmore[11], Steve Rintoul[16], Karl Safi[11], Philip Sutton[4], Robert Strzepek[17], Kim Tanneberger[2], Suzanne Turner[2], Anya Waite[18] & John Zeldis[10]

[1] National Institute of Water and Atmosphere, Centre for Chemical and Physical Oceanography, Department of Chemistry, University of Otago, Dunedin, New Zealand; [2] School of Environmental Sciences, University of East Anglia, Norwich NR4 7TJ, UK; [3] Plymouth Marine Laboratory, Prospect Place, The Hoe, Plymouth, Devon PL1 3DH, UK; [4] National Institute of Water and Atmosphere, Greta Point, PO Box 14-901, Wellington, New Zealand; [5] Antarctic Co-operative Research Centre, University of Tasmania, GPO Box 252-80, Hobart, Tasmania, 7001, Australia; [6] Department of Environmental Sciences,University of Plymouth, Drake Circus, Plymouth PL4 8AA, UK; [7] Department of Marine Chemistry and Geochemistry MS25, Woods Hole Oceanographic Institute, Woods Hole, Massachusetts 02543, USA; [8] Netherlands Institute for Sea Research (NIOZ), Department of Marine Chemistry and Geology, Postbus 59, 1790 AB Den Burg – Texel, The Netherlands; [9] Department of Chemistry, University of Otago, PO Box 56, Dunedin, New Zealand; [10] National Institute of Water and Atmosphere, Christchurch, PO Box 8602, Christchurch, New Zealand; [11] National Institute of Water and Atmosphere, Hamilton, Box 11-115, Hamilton, New Zealand; [12] Institut fuer Meereskunde, Universitaet Kiel, Duesternbrooker Weg 20 D-24105 Kiel, Germany; [13] Biology Department, McGill University, 1205 Avenue, Dr. Penfield, Montreal, PQ H2T 2V8, Canada; [15] Department of Biological Sciences, Bowling Green State University, Bowling Green, Ohio 43403, USA; [16] CSIRO Division of Marine Research, GPO Box 1538, Hobart, Tasmania, 7001, Australia; [17] University of British Columbia, Departments of Botany and Oceanography, 6270 University Boulevard, Vancouver, BC, Canada, V6T 1Z4; [18] Centre for Water Research, Department of Environmental Engineering, University of Western Australia, Nedlands 6907, Western Australia, Australia.

Changes in iron supply to oceanic plankton are thought to have a significant effect on concentrations of atmospheric carbon dioxide by altering rates of carbon sequestration, a theory known as the 'iron hypothesis'. For this reason, it is important to understand the response of pelagic biota to increased iron supply. Here we report the results of a mesoscale iron fertilization experiment in the polar Southern Ocean, where the potential to sequester iron-elevated algal carbon is probably greatest. Increased iron supply led to elevated phytoplankton biomass and rates of photosynthesis in surface waters, causing a large drawdown of carbon dioxide and macronutrients, and elevated dimethyl sulphide levels after 13 days. This drawdown was mostly due to the proliferation of diatom stocks. But downward export of biogenic carbon was not increased. Moreover, satellite observations of this massive bloom 30 days later, suggest that a sufficient proportion of the added iron was retained in surface waters. Our findings demonstrate that iron supply controls phytoplankton growth and community composition during summer in these polar Southern Ocean waters, but the fate of algal carbon remains unknown and depends on the interplay between the processes controlling export, remineralisation and timescales of water mass subduction.

The supply of iron, via dust, to the ocean in the past is thought to have differed significantly from that of the present day[1], and may alter again in the near future owing to the additional influence of anthropogenic changes in aridity and hence dust flux[2]. Such variations in iron supply are thought to alter the magnitude of oceanic primary[2] and export[1] production and the subsequent uptake of atmospheric CO_2. Mesoscale iron-enrichment of the ocean (Ironex II, 3.5 °S, 105° W)[3] showed that iron supply controls phytoplankton processes[4] in the high-nitrate low-chlorophyll (HNLC) equatorial Pacific Ocean, resulting in enhanced algal stocks[3] and associated macronutrient uptake[3] and CO_2 drawdown[5]. However, modelling simulations of the effect of iron fertilization on equatorial Pacific waters indicate that it is unlikely to be a significant region for iron-mediated carbon sequestration[6]. In contrast, the Southern Ocean is the largest repository of unused macronutrients in surface waters[5], and an important region for intermediate- and deep-water formation; consequently, it is a potential site for enhanced sequestration of carbon[5,6].

The Southern Ocean is thought to have a disproportionate influence on the functioning of the global carbon cycle in both the present[7] and the geological past[8]. Indeed, palaeoceanographic proxies suggest that export production during the Last Glacial Maximum was increased in these waters, probably due to increased iron supply[9]. Today, much of this region is characterized by low iron levels and/or deep mixed layers[10] where iron[10,11], light[12,13] or iron/light co-limitation[14] may control phytoplankton growth rates. Silicate availability, particularly during summer, may determine diatom growth rates (V. Franck, personal communication) and nothing is known about the response of large grazers[15] to increased algal stocks. These issues were addressed by conducting the *in situ* mesoscale Southern Ocean iron-release experiment (SOIREE) over 13 days in February 1999 (Fig. 1a). SOIREE confirms that iron supply controls phytoplankton processes at this site in summer, but as no significant iron-increased export production was observed we could not test the second tenet of the 'iron hypothesis'[1], which requires that fixed carbon is then sequestered in the deep ocean.

Site selection and survey

The Southern Ocean is characterized by several circumpolar fronts, which separate regions of relatively uniform water-mass properties[16] and coincide with strong current cores of the Antarctic Circumpolar Current (ACC)[17]. Mixed-layer depth generally decreases (Fig. 1a), and macro-nutrient levels increase[18], from north to south in this region. The SOIREE site (61° S, 140° E) was chosen to be representative of the properties (such as mixed-layer depth, Fig. 1a) of a broad region of circumpolar HNLC waters, yet have sufficiently low

[14] Present address: School of Marine Sciences, University of Maine, Orono, Maine 04469, USA.

horizontal current shear to maximize the time that fertilized waters could be tracked. Before SOIREE we made a transect about 115 km northwards on the 139° E meridian (that is, upstream of the likely site) and about 30 km east to west, to constrain spatial variability and finalize site selection. Hydrographic and expendable bathythermograph (XBT) results indicated a buoyant seasonal mixed layer of about 65 m depth (Fig. 1b), as suggested by climatological data sets (Fig. 1a), and clear zonal similarity to hydrographic[19] and XBT[20] sections.

Mixed-layer nitrate (~25 ± 1 μM)[18] and phosphate (~1.5 ± 0.2 μM) levels were relatively high, silicate (~10 ± 0.4 μM)[18] was intermediate, and dissolved iron levels were low (~0.08 ± 0.03 nM)[10], for polar waters. Chlorophyll *a* concentration was 0.25 mg m^{-3}, and dominated by pico-eukaryotes (~50% chlorophyll *a*, see Methods),

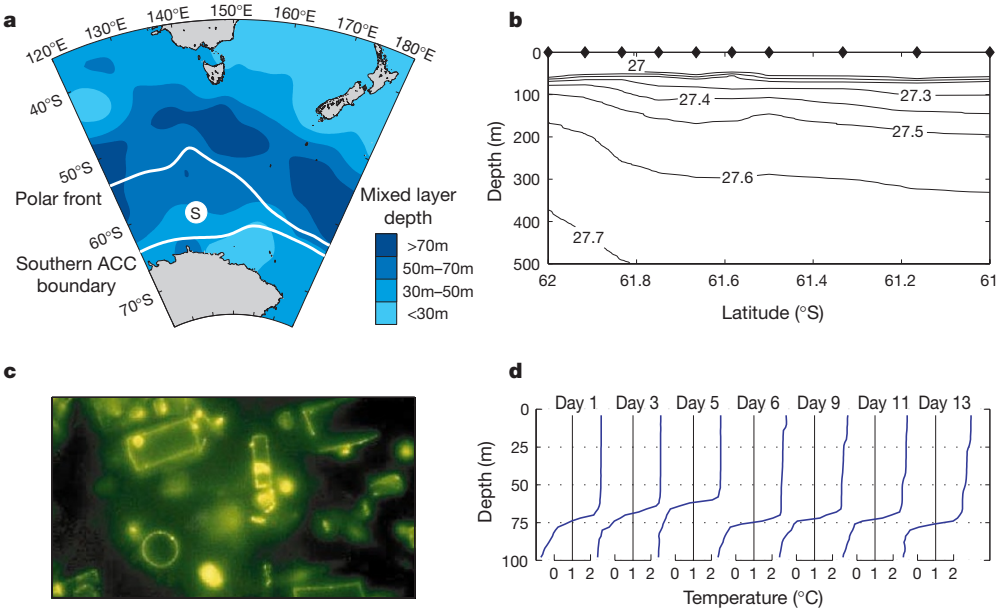

Figure 1 Site selection, pre-release survey and water-column structure. **a**, Summer mean mixed-layer depth—calculated from the World Ocean Atlas database—for the Australian–Pacific sector of the Southern Ocean. The location of the experiment (letter S), and the positions of the main circumpolar features are shown. ACC, Antarctic Circumpolar Current. **b**, Upper-ocean density-anomaly section (contours, kg m^{-3}) along the 139° E meridian during the survey before SOIREE. Contouring is based on 10 CTD casts (filled diamonds). **c**, Photomicrograph of diatoms (width of image, 350 μm) from surrounding HNLC waters (10 m depth) on 12 February 1999. The green fluorescence indicates iron-stressed diatoms (flavodoxin immunofluorescence assay[21]). **d**, Temporal evolution of vertical temperature structure within the patch (surrounding HNLC waters also exhibited these trends).

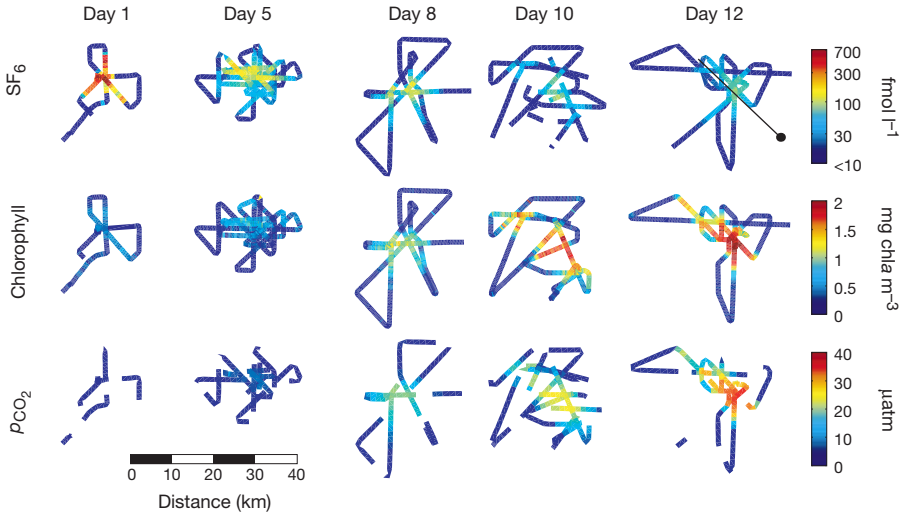

Figure 2 Temporal evolution of physical, chemical and biological properties during SOIREE. The figure shows maps of subsurface (5 m depth) SF_6 concentrations (top row), chlorophyll *a* concentrations (middle row), and changes in partial pressure of CO_2 (p_{CO2}; bottom row) within the iron-fertilized waters, relative to outside the patch. Taking into account changes in the area of the patch, the upper limit of spatial variability of SF_6, chlorophyll *a* and p_{CO2} levels within the patch was estimated to <15%, <20% and <10% of the daily mean value, respectively. The sensitivity of the SF_6 analytical system was ten times lower than the background signal, the precision and limit of detection of the chlorophyll *a* method was 0.04 and 0.01 mg m^{-3}, respectively, and both the accuracy and precision of the p_{CO2} measurements was ~1 μatm. The 'ribbon' plots denote the vessel track during the daily SF_6 surveys, and the expanding patch size with time. The solid line in the SF_6 plot (day 12) is the location of the southwest–northeast CTD transect through the patch on 22 February (day 13) shown in Fig. 4. The patch moved no more than ~10 km d^{-1} to the northeast, then later to the southeast, and the patch area (based on a linear fit) increased by ~15 km^2 d^{-1}.

with an 'inoculum' of diatoms (~20% chlorophyll *a*). Cells exhibited low values of photosynthetic competence (F_v/F_m = 0.22) and the resident large diatoms contained flavodoxin, a protein present under iron-stressed conditions[21] (Fig. 1c), both suggesting iron-limitation. Thus, we had favourable conditions for determining a response to iron-enrichment. We started SOIREE south of the polar front and north of the Southern ACC front (Fig. 1a), in a 65-m mixed layer (Fig. 1d) on 9 February 1999. Occupation of the site ended on 22 February (day 13). Times are in UTC (that is, GMT), and day 1 is defined as the 24-h period starting at 12:00 UTC, 9 February.

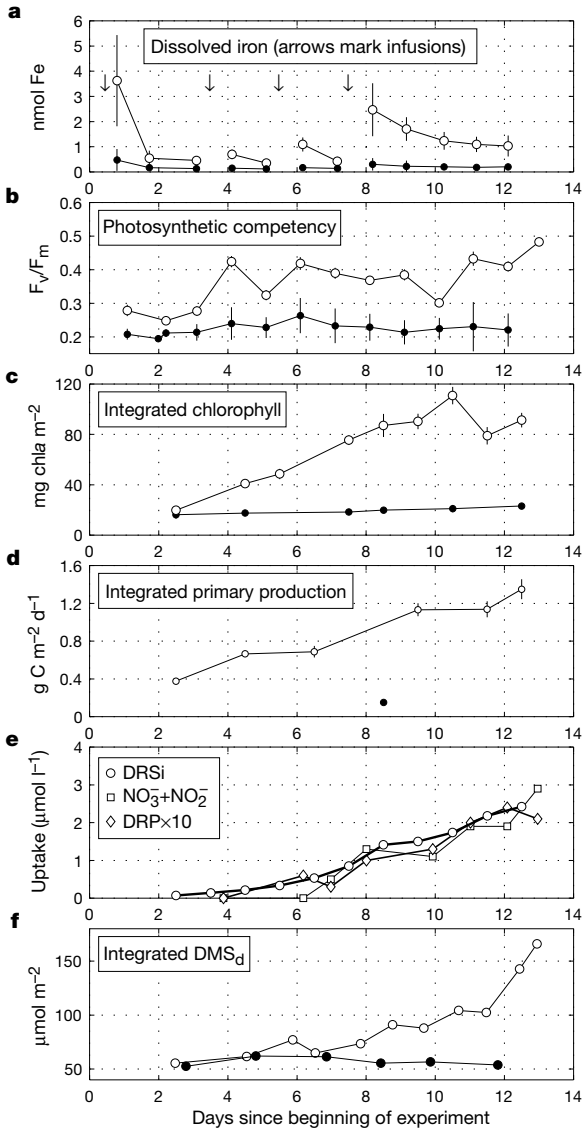

Figure 3 Time-series measurements made during SOIREE. Open and filled symbols show measurements made respectively inside and outside iron-fertilized waters. Underway data are expressed as the daily mean value for inside (defined as >50% of the peak SF_6 levels on that day) and outside the patch (defined as <10 fmol l^{-1}). Error estimates are expressed as ± 1 standard deviation of the mean for underway data (**a**, **b** and **e**) and ± 1 standard error of the mean for the discrete data (**c**, **d** and **f**). The range of sample sizes during SOIREE is provided in parentheses: **a**, underway sampling of dissolved iron levels (n = 5–17 (in); 9–29 (out)) in surface waters (~3 m) and the timing of the four iron infusions; **b**, underway sampling (~5 m) of community photosynthetic competency (F_v/F_m) (n = 8–40 (in); 6–84 (out)); **c**, column-integrated chlorophyll *a* (six depths, 0–65 m, n = 3 pseudo-replicates); **d**, column-integrated primary production (six depths, 0–65 m, n = 3 pseudo-replicates); **e**, macronutrient uptake (silicate: from ^{32}Si uptake[33], n = 2 pseudo-replicates, error always <10% of the mean), nitrate and phosphate depletion (underway sampling (~5 m), n = 12–18 (in); 14–34 (out), the greatest spatial variability was <15% of the standard deviation of the mean), DRSi is dissolved reactive silica, DRP is dissolved reactive phosphorus; **f**, column-integrated DMS (six depths, 0–65 m, n = 3 pseudo-replicates, errors are all smaller than the symbol size). Nitrate and phosphate depletion was obtained by subtraction of levels within the patch from levels in the surrounding waters (which exhibited no significant change in during SOIREE).

The experiment

Surface waters were fertilized with iron following an approach[22]—employed in Ironex I[23] and II[3]—that added a conservative tracer sulphur hexafluoride (SF_6)[24] concurrently to provide rapid identification of iron-enriched waters. The release of iron and SF_6 over an area of ~50 km^2 increased levels of SF_6 and dissolved iron to 300 fmol l^{-1} (mean) and ~3 nM, respectively (Figs 2 and 3a). Daily mapping of the spatial extent of labelled waters (that is, the patch) indicated that they had mixed in—within 48 h—to cover 100 km^2, increasing to ~200 km^2 by day 13. SF_6 levels remained greater than 50 fmol l^{-1} throughout SOIREE (Fig. 2), and thus no further SF_6 was added. Interspersed between mapping, hydrographic stations within (at the patch centre) and outside the patch indicated little change in the physical structure of the upper ocean during days 1–4. Thus, trends in data obtained when the ship was underway (Fig. 2) were applicable over the upper 65 m. On days 5/6 and 8/9, relatively calm conditions led to the development of transient thermal structures within the seasonal mixed layer, both inside (Fig. 1d) and outside the patch. These features were eroded and mixed down to 40 m on days 10/11. Subsequent warming resulted in three temporary strata between 0 and 20 m, 20 and 50 m, and 50 and 65 m, within the seasonal mixed layer on day 13.

Daily surveys of dissolved iron revealed that after iron infusion no. 1, levels were initially increased (Fig. 3a), similar to those in the iron-rich regions of the Atlantic polar front[11], and comparable to concentrations during Ironex I[23] and II[3]. By day 2 levels of dissolved iron decreased rapidly, probably due both to the patch spreading, and to its conversion to particulate form, as total (unfiltered) iron levels remained at about 2 nM. Dissolved iron levels were used as the criterion to determine when to add more iron during SOIREE; three further infusions (nos 2, 3 and 4) were required on days 3, 5 and 7, respectively, when levels of dissolved iron decreased towards those of the surrounding waters (Fig. 3a). After the final infusion (no. 4) levels of dissolved iron again initially decreased, but then remained at about 1 nM until the end of the site occupation. We note that Fe(II)—estimated to have a half-life of less than 1.0 h for oxidation to Fe(III) in these waters[25]—was the predominant species on days 12/13. Based on our limited understanding of iron chemistry in the ocean[26], the high concentrations of Fe(II) and their persistence over several day/night cycles is best explained by a production mechanism (photoreduction) coupled with a maintenance mechanism (iron complexation), respectively. The existence of the latter mechanism is supported by a small data set (relative to that for Fe(II)) of Fe-binding ligand measurements; concentrations of such ligands remained at about 3.5 nM both inside and outside the patch until day 11, then increased to 8.5 nM inside the patch (P.C., unpublished data).

Bloom evolution

The first indication of an algal response to iron enrichment was a small but detectable increase in F_v/F_m after 24 h (Fig. 3b), with no change in the magnitude of algal stocks or production until days 3/4 (Fig. 3c and d). Subsequent sustained increases in both chlorophyll *a* and production rates in the patch were not reflected by trends in F_v/F_m, which increased immediately after each infusion, followed by a small decrease within 24 h (Fig. 3b). Although F_v/F_m increased by day 1, other physiological indices of the alleviation of algal iron stress—slower saturating rates of iron uptake (M.M., unpublished data), and decreases in diatom flavodoxin levels[21] and in algal sinking rates[27] (Table 1)—were not evident until days 5–7. This time lag suggests that cells initially allocated resources to components with

an obligate requirement for iron[28], reflecting different response times of physiological and biochemical processes to iron enrichment. Inside the patch, net algal growth (see Methods) increased from 0.08 ± 0.01 d^{-1} early in SOIREE to 0.19 ± 0.02 d^{-1} later in the study, that is, lower than in on-deck studies[10]. These elevated growth rates resulted in a sixfold increase in chlorophyll *a* (Fig. 2) whereas algal carbon tripled. Thus, ratios of carbon to chlorophyll *a* that were approximately 90 just before SOIREE halved by day 13 within the patch. Surveys of surrounding waters indicated no significant changes in properties during SOIREE (Figs 2 and 3).

In the upper ocean, properties such as particle attenuation (the effect of particle density on transmission of light through sea water) were initially vertically homogeneous within the patch, but became heterogeneous over time, exhibiting a subsurface maximum by day 13 (Fig. 4). This transition was attributed to the presence of thermal features after day 5 (Fig. 1d). Settling of large cells from the upper 20 m is unlikely to explain this heterogeneity, as their sinking rates decreased over time. Alternatively, the trapping of cells in this upper layer probably resulted in marked photoinhibition (relative F_v/F_o, a proxy for photoinhibition[29] (see Methods), was 0.5 on days 7/8), which cells at depths in excess of 20 m did not exhibit (relative $F_v/F_o > 1.0$). Modelling and experimental studies on Antarctic phytoplankton indicate that inhibition of photosynthesis by ultraviolet radiation is relatively high during such transient events[30]. Exposure to higher irradiances and elevated ultraviolet dosage may have depressed the F_v/F_m values of cells in surface waters, relative to those at depth (Fig. 4). Consequently, the magnitude of F_v/F_m from underway mapping may not be representative of cells at depth after day 5 (Fig. 3b).

Water column optics and the role of light availability

The development of the bloom resulted in reduced mean water-column light levels, reducing the photic depth I_o (nominally 1% of surface photosynthetically active radiation (PAR)), from 84 m (K_d = 0.055 m^{-1}, see Methods) to about 45 m (K_d = 0.105 m^{-1}) over 13 d. Such self-shading may have altered algal iron requirements during SOIREE[14,31], and can impose an upper limit on chlorophyll *a* levels[12,13]. An on-deck study (see Methods) investigated the effect of mixed-layer depth (see Fig. 1a), and thus mean irradiances, on iron-enriched phytoplankton. Although based on a limited number of samples, the '40 m' and '65 m' treatments both exhibited similar increases in chlorophyll *a* (Fig. 5) and macronutrient depletion (not shown) that were comparable to (in fact, twice) those measured *in situ*. In contrast, in the '100 m' treatment there was little increase in chlorophyll *a*: this suggests light limitation, or Fe/light co-limitation, of growth in waters with deep mixed layers.

Pelagic community response

The algal and heterotrophic communities responded differently to iron enrichment. Initial increases in chlorophyll *a* and cell abundance were due to pico-eukaryotes (Table 2), and abundances of autotrophic flagellate (mainly prymnesiophytes) increased between days 2 and 8. However, after day 6, there was a floristic shift to large diatoms, which were dominated by *Fragilariopsis kerguelenis* (30–50 μm cell length, 4.4×10^4 cells l^{-1} by day 12). The number of cells per chain for this species doubled to 14 by day 12 of SOIREE. Blooms of this species have been reported at the polar front in the Atlantic sector[32]. These floristic shifts probably mediated changes in the concentrations of climate-reactive gases in surface waters (see below). Moreover, iron supply to diatoms resulted in decreased Si:C uptake ratios[33], as observed previously in on-deck iron enrichments[34].

Between days 0 and 13 (Table 2), bacterial abundances changed little whereas production rates approximately tripled, suggesting significant rates of bacterivory. The timing of increases in bacterial production did not correspond to that of the initial iron enrichments, but followed increases in primary production (days 7–12). Ciliate abundances quadrupled by day 13 (Table 2), and microzooplankton herbivory was predominantly on cells smaller than 20 μm, with little evidence of grazing on large diatoms. Copepods were the dominant large grazers, with krill and salps rare and absent, respectively, in net hauls. The clearance rates of the copepods changed little, and although chlorophyll *a* increased inside the patch, resulting in elevated copepod ingestion rates, these remained relatively low. The dominance of the bloom by *F. kerguelenis*, a highly silicified diatom that may be morphologically adapted to minimize grazing[35], was probably responsible for low rates of diatom herbivory.

Biogeochemical response

Iron-increased primary production resulted in significant uptake of macronutrients (Fig. 3e), and decreases in both partial pressure of CO_2 (p_{CO2}; Fig. 2) and dissolved inorganic carbon (12–18 μmol kg^{-1})[33] from days 5/6 onwards. There was no significant change in dissolved nitrous oxide levels in the patch relative to the surrounding waters (data not shown). During SOIREE, large diatoms accounted for up to 75% of primary production (see Methods) and were probably responsible for most of the observed 35–40 μatm decrease in p_{CO2} (ref. 33). Particulate dimethylsulphoniopropionate (DMSPp; the algal precursor of dimethyl sulphide, DMS) levels had increased after day 3, whereas dissolved DMS (DMS_d) concentrations initially increased on day 8 within the patch, and had tripled by day 13 (Fig. 3f). In contrast to the mainly diatom-mediated shifts in p_{CO2}, other plankton are probably responsible for elevated DMS levels; increases in prymnesiophyte

Table 1 Particulate export and algal settling estimates during SOIREE

Time periods	Value in-patch/value outside-patch			
	Trap POC flux	Trap BSi flux	$^{234}Th:^{238}U$	Mean phytoplankton (>10 μm) sinking rates
Days 0–2	–	–	1.06 (±0.14)	1.31
Days 7–9	1.18	0.94	1.04 (±0.12)	0.70
Days 11–13	1.64	2.21	0.99 (±0.14)	0.57

POC and BSi denote downward particulate organic carbon and biogenic silica, respectively. All data are expressed as relative ratios of the magnitude of export estimates (at 100 m depth) and algal sinking rates (measured on samples from 5 m depth) inside and outside the iron-fertilized patch over time periods when free-drifting sediment traps were deployed. $^{234}Th:^{238}U$ represents the integrated (0–100 m) $^{234}Th:^{238}U$ activity ratio, expressed here as a relative in-patch/outside-patch difference and the associated error (± 1 standard error of the mean). Errors cannot be calculated for trap fluxes and algal sinking rates as only one datum was obtained from outside-patch stations per deployment.

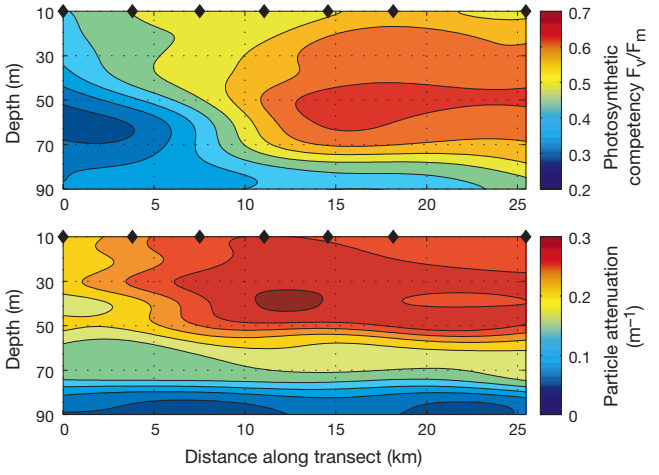

Figure 4 A vertical section (from the southeast to the northwest) through the iron-enriched patch on the night of 22 February. See SF_6 (day 12)) in Fig. 2 for transect location in relation to iron-fertilized waters. **a**, Photosynthetic competency (F_v/F_m), and **b,** particle attenuation (background attenuation due to seawater has been subtracted). The filled diamonds denote CTD casts.

abundances, and subsequent decreases—owing to elevated herbivory by microzooplankton—were coincident with marked increases in DMSPp (days 3–8), and in DMS (days 9–13), respectively (S.T., unpublished data). Laboratory studies have shown that the prymnesiophyte–microzooplankton pathway is particularly important in the production of DMSP and subsequent release of DMS[36]. Thus, upper-ocean concentrations of climate-reactive gases may be controlled by different algal taxa during iron-mediated blooms.

Particle export was estimated using surface-tethered free-drifting sediment traps, and the deficit of total dissolved and particulate ^{234}Th in the upper 100 m. There was no evidence of iron-increased particle export from the ^{234}Th data (Table 1). The trap collections exhibited greater export of particulate organic carbon and biogenic silica inside the patch than outside (Table 1). However, large variations in fluxes of particulate organic carbon (75%) and biogenic silica (17%) were recorded during two deployments outside the patch (days 0–2 and 11–13), suggesting that the apparent increases inside the patch could result from the inherent variability of the trapping methodology[37]. The decrease in algal sinking rates within iron-enriched waters, which has been observed in laboratory cultures when iron-depleted diatoms were iron-enriched[27], also supports the conclusion that there was no discernible increased export rates during the brief 13-d observation period.

Fate and longevity of the bloom

We now consider the physiological status of the algal community within the patch on day 13 of SOIREE. Algal F_v/F_m was sub-maximal in the upper 15 m (0.5; ref. 4), but maximal (0.65; ref. 4) at 50 m (Fig. 4), suggesting that cells were not resource-limited at depth. The high ambient nitrate and phosphate levels in surface waters were unlikely to limit growth, and there is indirect evidence from an on-deck experiment that cells were silicate-replete; the silicate uptake kinetics of the resident diatoms permitted silicate depletion to at least 4 μM, well below the ambient levels (> 6 μM) detected on day 13. Levels of dissolved iron on day 13 were ten times higher than in surrounding waters (Fig. 3a) yet the flavodoxin levels of diatoms (0–10 m) in iron-fertilized waters, which reached a minimum of about 50% of the initial value between days 5 and 8, increased after day 8 until the end of SOIREE.

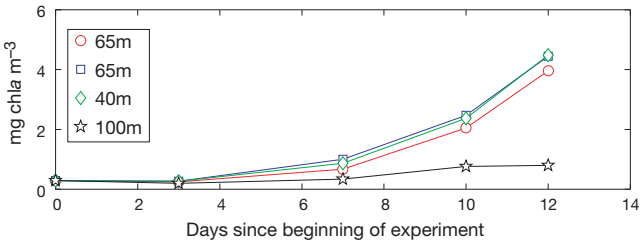

Figure 5 Changes in chlorophyll *a* levels with time during an on-deck iron/light perturbation experiment. Iron-enriched samples were incubated at a range of mean light levels simulating mixed-layer depths of 40 m (20% I_0), 65 m (10% I_0, two replicate carboys) and 100 m (5% I_0) (see Methods). The standard error of the mean of three pseudo-replicates from each carboy was <12% in all cases.

The cellular accumulation of flavodoxin[21] is particularly sensitive to algal iron stress, being detectable in cultured diatoms at 90% of maximum algal growth rates[38]. Moreover, flavodoxin and F_v/F_m respond to iron limitation on different timescales, and represent different classes of photosynthetic response. Any iron-mediated down-regulation of photosynthetic capacity, reflected by a reduction in F_v/F_m, is likely to be delayed until all other compensatory mechanisms to reduce cellular iron requirements, such as flavodoxin accumulation, have been exploited[38]. The presence of flavodoxin suggests that bioavailable iron levels were sub-optimal on day 13, at least in the dominant diatom species. These conditions may have been caused by changes in the partitioning of iron between the inorganic and organic pools. Rates of iron uptake from siderophore-bound iron, which are enhanced in iron-limited cells[39], were faster towards the end of SOIREE (M.T.M., unpublished data), suggesting that cells were iron-stressed. In spite of increased algal iron stress, primary production rates were high, and by inference the bloom remained productive after day 13 (ref. 40).

Levels of chlorophyll *a* increased by more than six times during SOIREE, yet there were no significant concomitant increases in the magnitude of loss processes, with small losses to the grazer and export routes (Tables 1 and 2). Thus, at the patch centre the accumulation of algal carbon (4.1 g C m^{-2}, see Methods) accounted for approximately 67% of iron-increased primary production (6.1 g C m^{-2}, see Fig. 3d). Application of these data to the 200-km^2 patch provides an upper estimate of carbon accumulation by day 13 (800 t algal C, see Methods) in response to the addition of about 1.7 t of iron. This is less than calculated by other methods[33], illustrating the uncertainties in making such estimates. On day 13, the 200-km^2 patch could potentially be distinguished from surrounding HNLC waters using SeaWiFS 1-km-resolution Ocean Color satellite data. On 21/22 March 1999, a SeaWiFS image showed a prominent ribbon-shaped feature (about 1,100 km^2) with estimated chlorophyll *a* concentrations of up to 3 mg m^{-3} (ref. 40). Calculations of the physical and biological evolution of the patch after our departure, and its geographical proximity to the location of the SOIREE patch on 22 February, suggest that the provenance of this feature is the iron-fertilized bloom[40]. This may alter the magnitude of biogeochemical signals such as p_{CO2} drawdown within this feature, relative to the amount of iron added. The accumulation of algal carbon in the bloom by late March may be considerably larger than estimated on day 13 (ref. 40).

SOIREE and the iron hypothesis

The 'ecumenical iron hypothesis'[41] summarizes our understanding of the relative roles of iron supply, uptake, algal growth and community structure, and grazing in the functioning of HNLC regions. Confirmation of this hypothesis[41] in Southern Ocean waters may be difficult, because light[12,13], iron/light co-limitation[14], or iron and silicate availability (V. Franck, personal communication) may also exert control on phytoplankton processes. At the onset of SOIREE, owing to the presence of a relatively deep mixed layer and intermediate silicate concentrations, we could not discount the influence of such factors on algal growth at this site. However, indirect evidence from *in situ* and on-ship observations

Table 2 Response of the microbial and metazoan communities during SOIREE

Parameter	Inside-patch abundances and rates	Outside-patch abundances and rates
Heterotrophic bacterial abundance	(4 ± 0.1) × 10^8 cells l^{-1}	(3 ± 0.1) × 10^8 cells l^{-1}
Heterotrophic bacterial production	(50 ± 8) ng C l^{-1} h^{-1}	(20 ± 2) ng C l^{-1} h^{-1}
Heterotrophic ciliate abundance	(13 ± 4.6) × 10^2 l^{-1}	(3 ± 0.5) × 10^2 l^{-1}
Pico-eukaryote abundance	(17 ± 2.9) × 10^6 l^{-1}	(5 ± 0.6) × 10^6 l^{-1}
Mesozooplankton stocks (0–70 m)	(2.0 ± 0.59) g C m^{-2}	(1.6 ± 0.86) g C m^{-2}
Mesozooplankton herbivory* (0–65 m)	(0.7 ± 0.12) % chlorophyll *a* cleared d^{-1}	(0.7 ± 0.28) % chlorophyll *a* cleared d^{-1}

*Estimated using gut fluorescence[50]. 'Inside-patch' denotes the highest daily mean (and standard error of the mean, based on at least three pseudo-replicates) of the abundances or rates observed in iron-fertilized waters during SOIREE. 'Outside-patch' denotes mean and standard error of abundances or rates (n > 3) for all days sampled. No significant changes in bacterial or meso- and micro-zooplankton abundances or activity were recorded in the surrounding waters. A comparison of day- and night-time mesozooplankton net hauls provided no evidence of arrested vertical migration within the patch relative to outside.

ruled out irradiance and silicate supply as significant factors during the 13-d study. During SOIREE, significant increases in algal F_v/F_m, growth, stocks and production rates provide unequivocal evidence of the role of iron in controlling the magnitude of phytoplankton processes. Moreover, iron supply—in conjunction with grazer dynamics—led to floristic shifts that resulted in a diatom-dominated bloom. These findings confirm the ecumenical iron hypothesis[41] for this site in summer. Although iron-mediated increases in primary production and a floristic shift to large diatoms will tend to elevate export production rates[42], this was not observed during our brief site occupation. Therefore, the second tenet of Martin's iron hypothesis[1]—regarding iron supply and the subsequent enhancement of downward particulate organic carbon export—could not be confirmed.

Extrapolation to Southern Ocean waters

We will now put the SOIREE results into a wider context. Although Southern Ocean waters are characterized by strong meridional gradients[16], the SOIREE site (65-m mixed layer; silicate, 10 μM) is broadly representative of more than 75% of polar waters in the Australian–Pacific sector of the Southern Ocean in summer (see Fig. 1a). Thus, our main finding—iron supply controls phytoplankton growth—may be cautiously applied to these waters. The ability to relate our findings, for summer, to other Southern Ocean sectors will require information on mixed-layer depth[43] (see Fig. 5) and on the relationship between ambient silicate levels and algal silicate uptake kinetics[14].

Geochemical models of sustained iron enrichment of the Southern Ocean[44], in the absence of data, assume an algal growth season of 3–12 months. SOIREE was conducted in late summer, when irradiances[45] and silicate levels[18] are less than those in December; mixed-layer depths are[20,46] similar to those in December. Thus, iron supply will probably control algal growth, under ambient conditions, during summer at this site. Evidence of continued growth[40] during March—despite incident irradiances of 50% of December levels[13]—suggests the 'iron-limited' growth season may be up to 4 months before irradiances severely limit algal growth. Based on silicate uptake over 13 d (3 μM, Fig. 3e) and winter reserve levels (20 μM)[18] at this site, silicate supply will probably influence algal growth rates under a simulated season of iron enrichment[44]. Furthermore, iron-mediated shifts in carbon/silicate uptake stoichiometry during SOIREE are an important determinant of the magnitude of carbon sequestration predicted by a modelling study of iron enrichment of the Southern Ocean in the geological past[33].

Southern Ocean bloom dynamics

Iron-increased chlorophyll *a* concentrations (more than 2 mg m^{-3}) during SOIREE are similar to those observed for polar front blooms from both vessel[11] and remote-sensing[47] surveys. Furthermore, the 13-d timescale required to attain 2 mg chl*a* m^{-3} during SOIREE is comparable to that estimated for blooms at the polar front using remote sensing[47]. There has been much debate about what factors limit algal biomass in the open Southern Ocean[1,10,11], but less about what sets an upper limit for chlorophyll *a* levels. Bio-optical models[12,13] predict an upper limit for chlorophyll *a* accumulation (1 mg m^{-3}) in the deep mixed layers (deeper than 60 m) near the polar front. Yet there is evidence from remote-sensing archives[47] of higher chlorophyll *a* levels (1.5–4 mg m^{-3}) for these waters than predicted[12,13]. The findings of SOIREE permit a re-evaluation of these modelling studies. Although they[12,13] could not consider the effects of iron supply on algal processes, Nelson and Smith[13] indicate the importance of the magnitude of loss processes in setting the critical depth, and the subsequent relationship between mixed layer and critical depths. Based on our findings, iron-enrichment by reducing the magnitude of loss processes—both directly (decreasing algal sinking rates) and indirectly (floristic shifts to taxa less prone to grazing[35])—permits chlorophyll *a* accumulation of greater than 1 mg m^{-3}.

Remotely sensed observations near the polar front[47] provide information on the geographical extent and timescales of algal blooms in polar waters. However, little is known about what determines the longevity of blooms in open Southern Ocean waters. The presence of high chlorophyll *a* concentrations more than 40 d after the onset of SOIREE raises fundamental questions about the mechanisms for the sustenance and longevity of this bloom. It is possible that the relatively short length scale of artificial relative to natural fertilization events may result in artefacts, such as the entrainment of silicate-rich waters as the SOIREE patch spread[40], that may have influenced bloom longevity. Nevertheless, a comparison of calculated algal iron requirements and iron levels within the SOIREE patch over 40 d indicate that biomass accumulation was sustainable[40]. The mechanisms by which sufficient Fe, via recycling or retention within surface waters and/or biota, was maintained to permit continued algal growth are unclear. However, the ability of resident cells to access this pool of organically bound iron only partially may have contributed to such longevity (M.T.M., unpublished data).

Future studies

The findings of SOIREE confirm the 'ecumenical iron hypothesis'[41] at this site in summer, and provide insights into the role of iron supply on bloom dynamics in the Southern Ocean. However, despite direct monitoring of the SOIREE bloom for 13 d, and indirectly[40] for a further 30 d, we can only speculate as to the fate—whether via export, remineralization and/or subduction—of the accumulated algal carbon. Thus, although we are able to justify relating our main findings to other periods of summer at this location, and to other polar waters, we cannot extrapolate them to longer-term sequestration of carbon in the Southern Ocean. Owing to the exchange of iron-fertilized and HNLC waters[40], SOIREE may be likened to a laboratory-culture chemostat in which silicate was added continuously, large diatoms were 'washed out'—resulting in both decreases in cell abundances (see ref. 48) and self-shading[12,13]—yet iron levels were always sufficient to permit net algal growth. It is not possible to determine whether the longevity of the bloom, and hence the potential delay in the onset of enhanced export of particulate organic carbon, was due to such an exchange of waters and/or to the maintenance of increased concentrations of dissolved iron. In order to examine the role of iron supply on the magnitude of downward fluxes of particulate organic carbon, the design of future studies will need to address these uncertainties. Furthermore, other approaches—such as modelling—will be required to constrain better the role of subduction in the eventual fate of iron-increased algal carbon in the Southern Ocean. □

Methods

Site selection and survey

Examination of climatological data sets (such as bathymetry, mixed-layer depth, buoy drift trajectories), and repeat hydrographic[19] and XBT sections[20] suggested that 61° S, 140° E was a potential site. Satellite sea surface height and Ocean Colour observations indicated that in January 1999 this region had low eddy activity and low chlorophyll *a* levels. XBT sections (RV *Astrolab*) along ~142° E, obtained 30 d and 14 d before SOIREE, re-confirmed the geographical location of the main frontal boundaries. During our pre-release survey, chlorophyll *a*, F_v/F_m and macronutrients were sampled from the vessel's non-toxic seawater supply (intake 5 m subsurface) and analysed[14] respectively by fluorometry (calibrated periodically with discrete chlorophyll *a* samples, corrected for quenching during daylight hours), fast-repetition-rate fluorometry , samples dark-adapted for 5 min), and using automated nutrient analysis. Underway samples for dissolved iron were obtained using a towed fish sampler, and were drawn from the vessel's non-toxic seawater system for p_{CO_2}. Samples for the single-cell and community flavodoxin assay[21] were pre-concentrated on board the vessel and analysed on land. There are several caveats associated with this assay[14].

Initiation of the SF_6/Fe patch

The SF_6 solution (~0.32 mmol l^{-1}) was prepared on the outward transit leg by saturating

4,000-litre tanks of sea water with pure SF_6 (ref. 24). During infusion no. 1, 3,600 litres of sea water containing ~165 g (1.1 mol) SF_6 were mixed with ~28,000 litres of sea water containing 3,813 kg $FeSO_4{\cdot}7H_2O$(ref. 24) using a dosing unit to control the mixing and pumping rate of Fe/SF_6 into surface waters (at ~15-m depth using a depressor). The release was co-ordinated within a lagrangian framework to account for surface water advection[24]. A WOCE-type surface drifting buoy attached to a holey-sock drogue centred at 30 m depth and fitted with GPS and argos was used to mark the centre-point of the patch[24]. The buoy position was updated every 10 min by UHF radio link[24]. The release track was based upon an expanding hexagon around the centre-point with track spacings at 600-m intervals, and a ship speed of 2–3 knots. SF_6 concentrations were analysed during daily underway mapping of the patch (5 m subsurface, vessel's non-toxic seawater system) and from vertical profiles taken from daily hydro-casts[49]. During infusion no. 1, the iron sulphate added to the upper ocean resulted in a theoretical addition of 3.8 nM Fe in a 50 km^2 patch. For infusions nos 2 and 3, 1,550 kg $FeSO_4{\cdot}7H_2O$ (in 12,000 litres of acidified seawater) was added each time (theoretical addition 2.6 nM Fe), and during the final infusion (no. 4) 1,750 kg $FeSO_4{\cdot}7H_2O$ (in 8,000 litres of acidified sea water) was added (theoretical addition 2.5 nM Fe).

Hydrographic sampling

The upper 150 m was sampled vertically (6–8 depths) each day using 12 acid-cleaned 10-litre bottles on a CTD rosette system at the patch centre (determined by SF_6 levels) and in the surrounding waters. Real-time vertical profiling of temperature, salinity, transmissivity, F_v/F_m, chlorophyll *a* fluorescence and underwater irradiance (PAR, 380–700 nm)[14] was performed. The attenuation coefficient (K_d) for PAR is not constant with depth in the upper ocean and was obtained by curve-fitting. F_v/F_o, an algebraic transform of $F_v/F_{m,,}$ was obtained from vertical fast-repetition-rate fluorometry casts. Discrete water samples were analysed for chlorophyll *a* (size-fractionated; >20, 5–20, 2–5 and 0.2–2 μm)[14], heterotrophic bacterial abundance[50], microzooplankton abundance[50], and phytoplankton abundance (see below)[50]. Additional samples were incubated on deck to measure rates of primary production (^{14}C, 24-h incubation, simulated *in situ*, size-fractionated as for chlorophyll *a*)[14], bacterial production[50], and microzooplankton grazing[50]. Estimates of cell size for each algal group in conjunction with size-fractionated chlorophyll *a* production were used to assess the contribution of algal taxa to community biomass or production. Mesozooplankton abundance was assessed from vertical hauls[50] from which additional animals were obtained and used, after 24 h acclimation, in herbivory experiments[50]. The Th:U activity ratio of particles in the upper ocean were collected using a submersible pumping system.

On-deck perturbation experiments

Water for an iron/light experiment was collected on 10 February from the patch centre (dissolved iron, 2 nM) using 30-litre clean Go-Flo samplers[51]. Sea water was added to clean[51] 25-litre polycarbonate carboys, within a clean air (class 100) environment, which were then shaded with neutral density screening to simulate the calculated mean light levels (see caveats[52]) in a 40-, 65- or 100-m mixed layer. Carboys were incubated in Perspex vessels (at ~2 °C) for 12 d, and periodically subsampled (class 100 environment). Subsamples were analysed for chlorophyll *a* and macronutrient levels.

Algal carbon accumulation, C:chlorophyll *a*, and growth rates

Algal cells from four depths (0–65 m) at the patch centre were identified, enumerated and sized using light (diatoms/dinoflagellates) or epifluorescence (autotrophic flagellates) microscopy, and flow cytometry (pico-eukaryotes, verified with epifluorescence microscopy), then converted to biovolume and cellular carbon using size and taxon-specific factors[53]. Algal carbon was integrated over the 65-m mixed layer. The accumulation of algal carbon during SOIREE was obtained by subtracting the column-integral on day 13 from that at the onset. Extrapolation of column-integrated algal carbon from the patch centre to the 200-km^2 patch yielded an upper limit of algal C accumulation during SOIREE (800 t C). However, if algal carbon was distributed throughout the patch in the same manner as SF_6, this estimate would be ~400 t C. Algal C and primary production data were used to estimate algal net growth rates[54] by comparing the cumulative iron-mediated increase in column-integrated production over SOIREE to the column-integrated accumulation of algal C. Column-integrated chlorophyll *a* and algal carbon were used to provide C:chlorophyll *a* ratios.

Received 6 January; accepted 4 September 2000.

1. Martin, J. H. Glacial-interglacial CO_2 change: The iron hypothesis. *Paleoceanography* **5,** 1–13 (1990).
2. Falkowski, P. G., Barber, R. T. & Smetacek, V. Biogeochemical controls and feedbacks on ocean primary production. *Science* **281,** 200–206 (1998).
3. Coale, K. H. *et al.* A massive phytoplankton bloom induced by ecosystem-scale iron fertilization experiment in the equatorial Pacific Ocean. *Nature* **383,** 495–501 (1996).
4. Behrenfeld, M. J., Bale, A. J., Kolber, Z. S., Aiken, J. & Falkowski, P. G. Confirmation of iron limitation of phytoplankton photosynthesis in the equatorial Pacific Ocean. *Nature* **383,** 508–510 (1996).
5. Cooper, D. J., Watson, A. J. & Nightingale, P. D. Large decrease in ocean-surface CO_2 fugacity in response to *in situ* iron fertilization. *Nature* **383,** 511–513 (1996).
6. Sarmiento, J. L. & Orr, J. C. Three-dimensional simulations of the impact of Southern Ocean nutrient depletion on atmospheric CO_2 and ocean chemistry. *Limnol. Oceanogr.* **36,** 1928–1950 (1991).
7. Sarmiento, J. L., Hughes, T. M. C., Stouffer, R. J. & Manabe, S. Simulated response of the ocean carbon cycle to anthropogenic climate warming. *Nature* **393,** 245–249 (1998).
8. Broecker, W. S. & Henderson, G. M. The sequence of events surrounding termination II and their implications for the causes of glacial interglacial CO_2 changes. *Paleoceanography* **13,** 352–364 (1998).
9. Kumar, N. *et al.* Increased biological productivity and export production in the glacial Southern Ocean. *Nature* **378,** 675–680 (1995).
10. de Baar, H. J. W. & Boyd, P. W. in *The Dynamic Ocean Carbon Cycle: A Midterm Synthesis of the Joint Global Ocean Flux Study* Ch. 4 (eds Hanson, R. B., Ducklow, H. W. & Field, J. G.) 61–140 (International Geosphere Biosphere Programme Book Series, Cambridge Univ. Press, Cambridge, 1999).
11. de Baar, H. J. W. *et al.* Importance of iron for plankton blooms and carbon dioxide drawdown in the Southern Ocean. *Nature* **373,** 412–415 (1995).
12. Mitchell, B. G., Brody, E. A., Holm-Hansen, O., McClain, C. & Bishop, J. Light limitation of phytoplankton biomass and macronutrient utilization in the Southern Ocean. *Limnol. Oceanogr.* **36,** 1662–1677 (1991).
13. Nelson, D. M. & Smith, W. O. Jr Sverdrup revisited: Critical depths, maximum chlorophyll levels, and the control of Southern Ocean productivity by the irradiance-mixing regime. *Limnol. Oceanogr.* **36,** 1650–1661 (1991).
14. Boyd, P. W., LaRoche, J., Gall, M., Frew, R. & McKay, R. M. L. The role of iron, light and silicate in controlling algal biomass in sub-Antarctic waters SE of New Zealand. *J. Geophys. Res.* **104,** 13395–13408 (1999).
15. Banse, K. Iron availability, nitrate uptake and exportable new production in the subarctic Pacific. *J. Geophys. Res.* **96,** 741–748 (1991).
16. Orsi, A. H., Whitworth, T. W. & Nowlin, W. D. Jr On the meridional extent and fronts of the Antarctic Circumpolar Current. *Deep-Sea Res. I* **42,** 641–673 (1995).
17. Nowlin, W. D. Jr & Klinck, J. M. The physics of the Antarctic Circumpolar Current. *Rev. Geophys. Space Phys.* **24,** 469–491 (1986).
18. Zentara, S. J. & Kamykowski, D. Geographic variation in the relationship between silicic acid and nitrate in the South Pacific Ocean. *Deep-Sea Res. A* **28,** 455–465 (1981).
19. Rintoul, S. R. & Bullister, J. L. A late winter hydrographic section from Tasmania to Antarctica. *Deep-Sea Res. I* **46,** 1417–1454 (1999).
20. Rintoul, S. R., Donguy, J. R. & Roemmich, D. H. Seasonal evolution of upper ocean thermal structure between Tasmania and Antarctica. *Deep-Sea Res. I* **44,** 1185–1202 (1997).
21. LaRoche, J., Boyd, P. W., McKay, R. M. L. & Geider, R. J. Flavodoxin as an *in situ* marker for iron stress in phytoplankton. *Nature* **382,** 802–805 (1996).
22. Watson, A. J., Liss, P. S. & Duce, R. A. Design of a small-scale iron fertilisation experiment. *Limnol. Oceanogr.* **36,** 1960–1965 (1991).
23. Martin, J. H. *et al.* Testing the iron hypothesis in ecosystems of the equatorial Pacific Ocean. *Nature* **371,** 123–129 (1994).
24. Law, C. S., Watson, A. J., Liddicoat, M. I. & Stanton, T. Sulphur hexafluoride as a tracer of biogeochemical and physical processes in an open-ocean iron fertilisation experiment. *Deep-Sea Res. II* **45,** 977–994 (1998).
25. Millero, F. J., Sotolongo, S. & Izaguirre, M. The oxidation kinetics of Fe(II) in seawater. *Geochim. Cosmochim. Acta* **51,** 793–801 (1987).
26. Geider, R. J. Biological oceanography: complex lessons of iron uptake. *Nature* **400,** 815–816 (1999).
27. Muggli, D. L., Lecourt, M. & Harrison, P. J. Effects of iron and nitrogen source on the sinking rate, physiology and metal composition of an oceanic diatom from the subarctic Pacific. *Mar. Ecol. Prog. Ser.* **132,** 215–227 (1996).
28. Greene, R. M., Geider, R. J., Kolber, Z. & Falkowski, P. G. Iron-induced changes in light-harvesting and photochemical energy conversion processes in eukaryotic marine algae. *Plant Physiol.* **100,** 565–575 (1992).
29. Behrenfeld, M. J., Prasil, O., Kolber, Z. S., Babin, M. & Falkowski, P. G. Compensatory changes in photosystem II electron turnover rates protect photosynthesis from photoinhibition. *Photosynth. Res.* **58,** 259–268 (1999).
30. Neale, P. J., Davis, R. F. & Cullen, J. J. Interactive effects of ozone depletion and vertical mixing on photosynthesis of Antarctic phytoplankton. *Nature* **392,** 585–589 (1998).
31. Sunda, W. G. & Huntsman, S. A. Interrelated influence of iron, light and cell size on marine phytoplankton growth. *Nature* **390,** 389–392 (1997).
32. Laubscher, R. K., Perissinotto, R. & McQuaid, C. D. Phytoplankton production and biomass at frontal zones in the Atlantic Sector of the Southern Ocean. *Polar Biol.* **13,** 471–481 (1993).
33. Watson, A. J., Bakker, D. C. E., Ridgwell, A. J., Boyd, P. W. & Law, C. S. Effect of iron supply on Southern Ocean CO_2 uptake and implications for glacial atmospheric CO_2. *Nature* **407,** 730–733 (2000).
34. Hutchins, D. A. & Bruland, K. W. Iron limited diatom growth and Si:N uptake ratios in a coastal upwelling regime. *Nature* **393,** 561–564 (1998).
35. Verity, P. & Smetacek, V. Organism life cycles, predation, and the structure of marine pelagic ecosystems. *Mar. Ecol. Prog. Ser.* **130,** 277–293 (1996).
36. Wolfe, G. V., Steinke, M. & Kirst, G. O. Grazing-activated chemical defence in a unicellular marine alga. *Nature* **387,** 894–897 (1997).
37. Buesseler, K. O. Do upper-ocean sediment traps provide an accurate record of particle flux? *Nature* **353,** 420–423 (1991).
38. McKay, R. M. L., Geider, R. J. & LaRoche, J. Physiological and biochemical response of the photosynthetic apparatus of two marine diatoms to Fe stress. *Plant Physiol.* **114,** 615–622 (1997).
39. Maldonado, M. T. & Price, N. M. Utilization of iron bound to strong organic ligands by phytoplankton communities in the subarctic Pacific Ocean. *Deep-Sea Res. II* **46,** 2447–2474 (1999).
40. Abraham, E. R. *et al.* Importance of stirring in the development of an iron-fertilized phytoplankton bloom. *Nature* **407,** 727–730 (2000).
41. Morel, F. M. M., Reuter, J. G. & Price, N. M. Iron nutrition of phytoplankton and its possible importance in the ecology of ocean regions with high nutrient and low biomass. *Oceanography* **4,** 56–61 (1991).
42. Boyd, P. W. & Newton, P. P. Does planktonic community structure determine downward particulate organic carbon flux in different oceanic provinces. *Deep-Sea Res. I* **46,** 63–91 (1999).
43. Obata, A., J. Ishizaka & Endoh, M. Global verification of critical depth theory for phytoplankton blooms with climatological *in situ* temperature and satellite ocean color data. *J. Geophys. Res.* **101,** 20657–20667 (1998).
44. Peng, T.-H. & Broecker, W. S. Factors limiting the reduction of atmospheric CO_2 by iron fertilisation. *Limnol. Oceanogr.* **36,** 1919–1927 (1991).
45. Bishop, J. K. B. & Rossow, W. R. Spatial and temporal variability of global surface solar irradiance. *J. Geophys. Res.* **96,** 16839–16858 (1991).
46. Trenberth, K. E., Large, W. G. & Olson, J. G. The mean annual cycle in global ocean wind stress. *J. Phys. Oceanogr.* **20,** 1742–1760 (1990).

47. Moore, J. K. *et al.* SeaWiFS satellite ocean color data from the Southern Ocean. *Geophys. Res. Lett.* **26,** 1465–1468 (1999).
48. Jackson, G. A. A model of the formation of marine algal flocs by physical coagulation processes. *Deep-Sea Res.* **37,** 1197–1211 (1990).
49. Law, C. S., Watson, A. J. & Liddicoat, M. I. Automated vacuum analysis of sulphur hexafluoride in seawater; derivation of the atmospheric trend (1970-1993) and potential as a transient tracer. *Mar. Chem.* **48,** 57–69 (1994).
50. Bradford-Grieve, J. M. *et al.* Pelagic ecosystem structure and functioning in the Subtropical Front region east of New Zealand in austral winter and spring 1993. *J. Plank. Res.* **21,** 405–428 (1999).
51. Fitzwater, S. E., Knauer, G. A. & Martin, J. H. Metal contamination and its effect on primary production methods. *Limnol. Oceanogr.* **27,** 544–551 (1982).
52. Maldonado, M., Boyd, P. W., Price N. M. & Harrison, P. J. Co-limitation of phytoplankton by light and Fe during winter in the NE subarctic Pacific Ocean. *Deep-Sea Res. II* **46,** 2475–2486 (1999).
53. Montagnes, D. J. S, Berges, J. A., Harrison, P. J. & Taylor, F. J. R. Estimating carbon, nitrogen, protein and chlorophyll *a* from volume in marine phytoplankton. *Limnol. Oceanogr.* **39,** 1044–1060 (1994).
54. Popp, B. N., Parekh, P., Tilbrook, B., Bidigare, R. R. & Laws, E. A. Organic carbon $\delta^{13}C$ variations in sedimentary rocks as chemostratigraphic and paleoenvironmental tools. *Palaeoclimatol. Palaeoecol.* **132,** 119–132 (1997).

Acknowledgements

We thank the officers and crew of the RV *Tangaroa*, and the management and staff of the NIWA Vessel Management Company. We also acknowledge the provision of physical oceanographic data by J. Church, M. Morris, V. Strass, RV *Astrolab*, and J. Barth and T. Cowles. We also thank M. Walkington (CTD calibration), J. Aiken (instrument loan), P. Nightingale (argos reception for tracking buoys), S. Groom (near-time high resolution Ocean Color satellite images), NASA (SeaWiFS images), and the companies CEFIC (UK) and BHP (Australia) for their support. We acknowledge two grants from the UK NERC to S.T. (Advanced Fellowship Award), and to A.J.W. and C.S.L. (SOIREE). K.O.B. and M.C. were funded by the US NSF. M.T.M. was funded by the NSERC Canada and the Center for Environmental Bioinorganic Chemistry, Princeton, USA. P.C., A.J.W. and D.C.E.B. received a grant within CARUSO from the European Union. New Zealand scientists were funded by the Government PGSF fund for Antarctic Research. J. Cullen, K. Hunter and C. Hurd provided comments and advice that improved this manuscript.

Correspondence and requests for materials should be addressed to P.W.B. (e-mail: pboyd@alkali.otago.ac.nz).